

Phonon features in terahertz photoconductivity spectra due to data analysis artifact: A case study on organometallic halide perovskites

Chan La-o-vorakiat, Liang Cheng, Teddy Salim, Rudolph A. Marcus, Maria-Elisabeth Michel-Beyerle, Yeng Ming Lam, and Elbert E. M. Chia

Citation: *Appl. Phys. Lett.* **110**, 123901 (2017); doi: 10.1063/1.4978688

View online: <http://dx.doi.org/10.1063/1.4978688>

View Table of Contents: <http://aip.scitation.org/toc/apl/110/12>

Published by the [American Institute of Physics](#)

Articles you may be interested in

[Mechanical signatures of degradation of the photovoltaic perovskite CH₃NH₃PbI₃ upon water vapor exposure](#)
Appl. Phys. Lett. **110**, 121903121903 (2017); 10.1063/1.4978687

[Femtosecond-timescale buildup of electron mobility in GaAs observed via ultrabroadband transient terahertz spectroscopy](#)
Appl. Phys. Lett. **110**, 121102121102 (2017); 10.1063/1.4978648

[Macroscopic ferroelectricity and piezoelectricity in nanostructured NaNbO₃ ceramics](#)
Appl. Phys. Lett. **110**, 122901122901 (2017); 10.1063/1.4978904

[Chemically induced structural heterogeneities and their relationship with component dynamics in a binary metallic liquid](#)
Appl. Phys. Lett. **110**, 121902121902 (2017); 10.1063/1.4978392



THE WORLD'S RESOURCE FOR VARIABLE TEMPERATURE SOLID STATE CHARACTERIZATION



OPTICAL STUDIES SYSTEMS



SEEBECK STUDIES SYSTEMS



MICROPROBE STATIONS



HALL EFFECT STUDY SYSTEMS AND MAGNETS

WWW.MMR-TECH.COM

Phonon features in terahertz photoconductivity spectra due to data analysis artifact: A case study on organometallic halide perovskites

Chan La-o-vorakiat,^{1,2,a)} Liang Cheng,³ Teddy Salim,⁴ Rudolph A. Marcus,^{3,5} Maria-Elisabeth Michel-Beyerle,³ Yeng Ming Lam,⁴ and Elbert E. M. Chia^{3,b)}

¹Nanoscience and Nanotechnology Graduate Program, Faculty of Science, King Mongkut's University of Technology Thonburi (KMUTT), Bangkok 10140 Thailand

²Theoretical and Computational Science Center (TaCS), Faculty of Science, King Mongkut's University of Technology Thonburi (KMUTT), Bangkok 10140 Thailand

³Division of Physics and Applied Physics, School of Physical and Mathematical Sciences, Nanyang Technological University, Singapore 637371

⁴School of Materials Science and Engineering, Nanyang Technological University, Singapore 639798

⁵Noyes Laboratory, California Institute of Technology, Pasadena, California 91125, USA

(Received 27 December 2016; accepted 1 March 2017; published online 20 March 2017)

We propose a simple scenario where the superimposed phonon modes on the photoconductive spectra are experimental artifacts due to the invalid formula used in data analysis. By use of experimental and simulated data of $\text{CH}_3\text{NH}_3\text{PbI}_3$ perovskites as a case study, we demonstrate that a correction term must be included in the approximated thin-film formula used in the literature; otherwise, parts of the spectra with high background permittivity near the phonon-mode resonances might interfere with the transient photoconductivity. The implication of this work is not limited to perovskites but other materials with strong vibrational modes within the THz spectral range. Published by AIP Publishing. [<http://dx.doi.org/10.1063/1.4978688>]

In the past few years, time-resolved terahertz spectroscopy (TRTS) has helped advance the development of organometallic halide perovskite photovoltaics.^{1–4} It is among the key techniques for investigating the photophysics of the charge carriers, providing direct measurements of charge carrier density, mobility, recombination rate kinetics, diffusion length, disordered-induced back-scattering parameters, and intra-excitonic transition energy.^{5–15} Previous investigations of perovskites focus on the measurement of photoconductivity, defined as the transient change in conductivity spectra after an optical excitation. One can extract the material parameters related to the intrinsic properties of the photogenerated carriers, by fitting the photoconductivity spectra to physical models such as Drude or Lorentz models.

Beside the standard analysis, there were also reports of phonon modes superimposed on the real part of the photoconductivity spectra.^{5,6,10,11} The overlaid phonon modes coincide with the steady-state (i.e., without any optical excitation) THz-phonon absorption profile due to the vibration of metal-halide bonds in the perovskites.¹⁶ The magnitude of the phonon features also correlates with the strength of phonon absorption.¹¹ These observations led to a legitimate postulate that the appearance of phonon modes in the photoconductive spectra is related to the strong intrinsic coupling between the phonons and charge carriers in the perovskites. The argument has been used to support the phonon-assisted homogenous broadening in the photoluminescence spectra.^{17,18}

However, in this work, we argue that one needs to perform a more vigorous analysis of the THz time-domain data, in order to properly determine the existence of charge-

phonon coupling in the perovskites. The phonon structure could artificially appear on top of the photoconductivity spectrum due to the *invalidity* of the standard formula for TRTS data analysis

$$\Delta\tilde{\sigma}_{tf} = -\epsilon_0 \frac{c}{d} (1 + \tilde{n}_{sub}) \frac{\Delta\tilde{E}}{\tilde{E}_0}, \quad (1)$$

that was used to convert a measured quantity $\frac{\Delta\tilde{E}}{\tilde{E}_0}$, to the complex photoconductivity $\Delta\tilde{\sigma}_{tf}$ of the thin film (*tf*). Here, $\Delta\tilde{E}$ is the pump-induced change in the transmitted THz electric field, \tilde{E}_0 is the THz transmission on an unexcited sample, \tilde{n}_{sub} is the complex refractive index of the substrate, d is the sample thickness, c is the speed of light, and ϵ_0 is the permittivity. The formula is applicable to free-standing dielectric slabs without any substrate.^{19,20} However, at the end of this article, we show that it is also applicable to low- k dielectric films (small equilibrium dielectric constant $\tilde{\epsilon}_{eq}$) on a typical THz-transparent substrate (e.g., quartz or sapphire) by omitting the first-order correction, $\frac{\omega d}{c} (\tilde{\epsilon}_{eq} - \frac{\tilde{n}_{sub}^2 + 1}{2})$, which is small compared to the leading-order term, $(1 + \tilde{n}_{sub})$. This condition is normally satisfied in the perovskites due to the low background dielectric nature of the film, *except* at the parts with high permittivity, i.e., near the phonon-mode resonances. Consequently, the phonon structure could artificially appear in the calculated photoconductivity spectrum.

As a demonstration, we analyze three of our own experimental data sets from a perovskite thin film measured at 15, 80, and 180 K.⁷ We compare the results from (1) the thin-film equation (Eqs. (1) and (2)) the numerical inversion from the transmission equation^{21,22} (Eq. (3)). The complex optical conductivity calculated directly from the transmission function is susceptible to phase errors due to the determination of

^{a)}Electronic mail: chan.lao@kmutt.ac.th

^{b)}Electronic mail: elbertchia@ntu.edu.sg

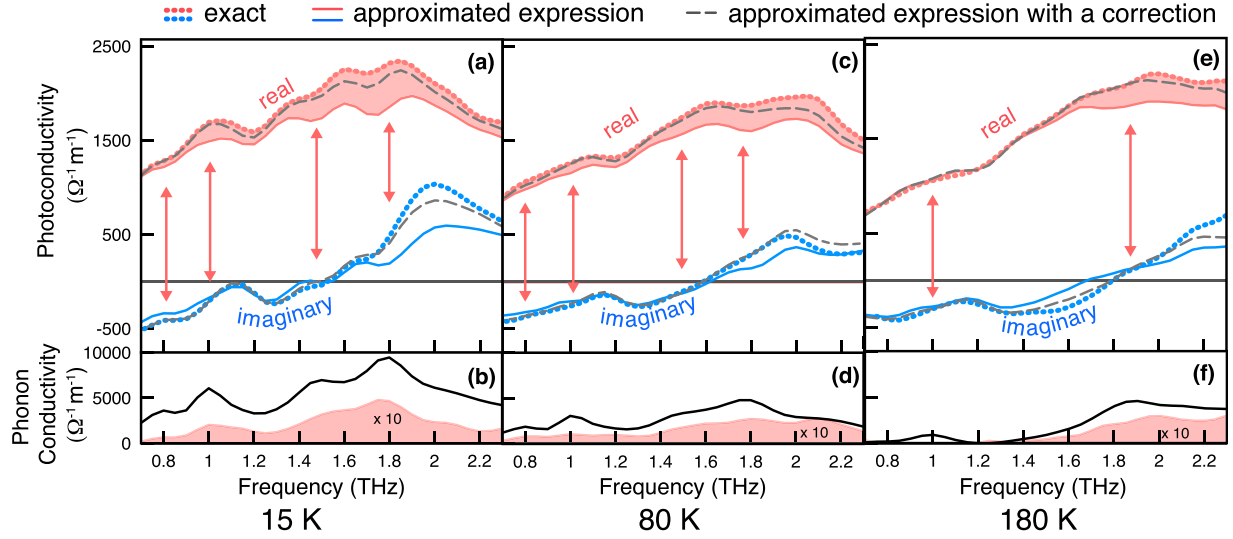


FIG. 1. The phonon spectral features overlaid on the photoconductivity of perovskite measured at 15, 80, and 180 K. (a), (c), and (e) The thin-film approximation used in the literature (Eq. (1), solid lines) underestimates the actual photoconductivity (dotted line) by the amount proportional to the phonon conductivity (shaded area). (b), (d), and (f) The errors in the real part of the photoconductivity (shaded area) are displayed alongside the corresponding steady-state phonon spectra (black line). The arrows indicate the modulations in photoconductivity at the phonon mode frequencies.

the substrate thicknesses.^{21,23} However, we have shown in the [supplementary material](#) that only the imaginary part suffers from such an uncertainty, and the real part of the optical conductivity can serve as a benchmark for the quality of the approximated expressions.

We noticed significant deviations from the exact photoconductivity at all temperatures. The errors in the real part of the photoconductivity indeed follow the feature of phonon modes and scales with the magnitude of steady-state phonon conductivities, as shown by the shaded areas in Fig. 1(b). The imaginary part of the photoconductivity shows a $\sim 50\%$ deviation around 2 THz (Fig. 1(a)). The deviation is understandable from the fact that the first-order correction, $\frac{\omega d \tilde{\epsilon}_{eq}}{c}$, is no longer a negligible fraction ($\sim 20\%$) of the photoconductivity expression due to the resonant behavior of the dielectric constant near the phonon modes (see Fig. 2).

Since our overlaid phonon features are embedded in the background structure of the photoconductivity as well as the

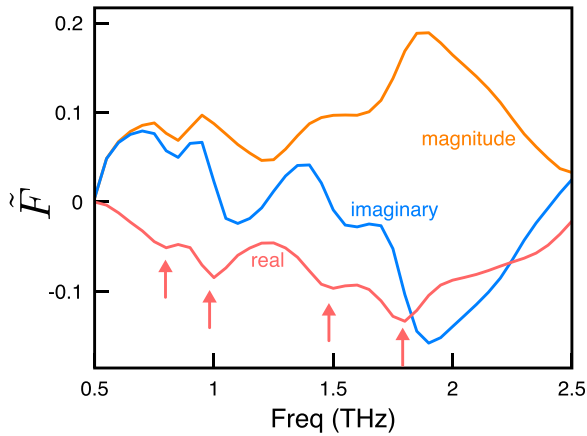


FIG. 2. The ratio of first order to zeroth order contributions of the photoconductivity expression, $\tilde{F} = \frac{i\omega d [\tilde{\epsilon}_{eq} - \frac{\tilde{n}_{sub}^2 + 1}{2}]}{c(1 + \tilde{n}_{sub})}$. The thickness of the film (d) is 230 nm, and the substrate refractive index (\tilde{n}_{sub}) is 2.1 for z-cut quartz. The analysis is performed on 15 K data (Fig. 1(a)). Phonon modes are indicated by the arrows.

measurement noise, we clarify our assertion by performing a numerical simulation based on a perovskite-like THz material. We set its conductivity as a sum of Lorentzian profiles centered near 1 and 2 THz with a transmission of about 90% at the peak (Fig. 3(a))—a realistic condition for the perovskites.¹⁶ Physically, the Lorentzian function represents phonon absorption.²⁰ As a response to an optical pump, we model the photo-generated free carriers in a material with a Drude-Smith-type photoconductivity, which is a consequence of carrier backscattering.^{7,24} With the help of the exact transmission equation (Eq. (3)), we calculate both the equilibrium and transient electric fields with the knowledge of the transmitted THz pulses through the substrate (obtained experimentally). We model two photoconductive responses from the experimental Drude-Smith parameters at 15 K and 180 K (compatible with Figs. 1(a) and 1(c)). The parameters are presented in the [supplementary material](#).

The simulation shows a noticeable deviation near the phonon peaks as expected (Fig. 3(c) in comparison to Fig. 3(b)), indicating that the thin-film approximation (Eq. (1)) is not necessarily a good representation of the transient photoconductivity near the phonon resonance frequencies. The extra feature appears as a modulation at the phonon mode frequency that was used as evidence of strong carrier-phonon coupling in the perovskites.^{5,6,10,11,17}

Next, to minimize the phonon artifact but keeping the simplicity of the algebraic formula in data analysis, we introduce a thin-film formula with a first-order correction term

$$\Delta \tilde{\sigma}_{ef}^{(1)} \approx -\epsilon_0 \frac{c \Delta \tilde{E}}{d \tilde{E}_0} \left\{ 1 + \tilde{n}_{sub} - \frac{i\omega d}{c} \left[\tilde{\epsilon}_{eq} - \frac{\tilde{n}_{sub}^2 + 1}{2} \right] \right\}, \quad (2)$$

where $\tilde{\epsilon}_{eq} = \tilde{n}_0^2$ is the equilibrium (i.e., no pump) refractive index of the film that is governed by phonon absorption. The new formula indeed improves the calculated conductivity especially near the phonon peaks (see Figs. 1(a), 1(c), and 1(e)). The drawback of the formula is that the film's equilibrium dielectric constant $\tilde{\epsilon}_{eq}$ has to be predetermined. Due to the

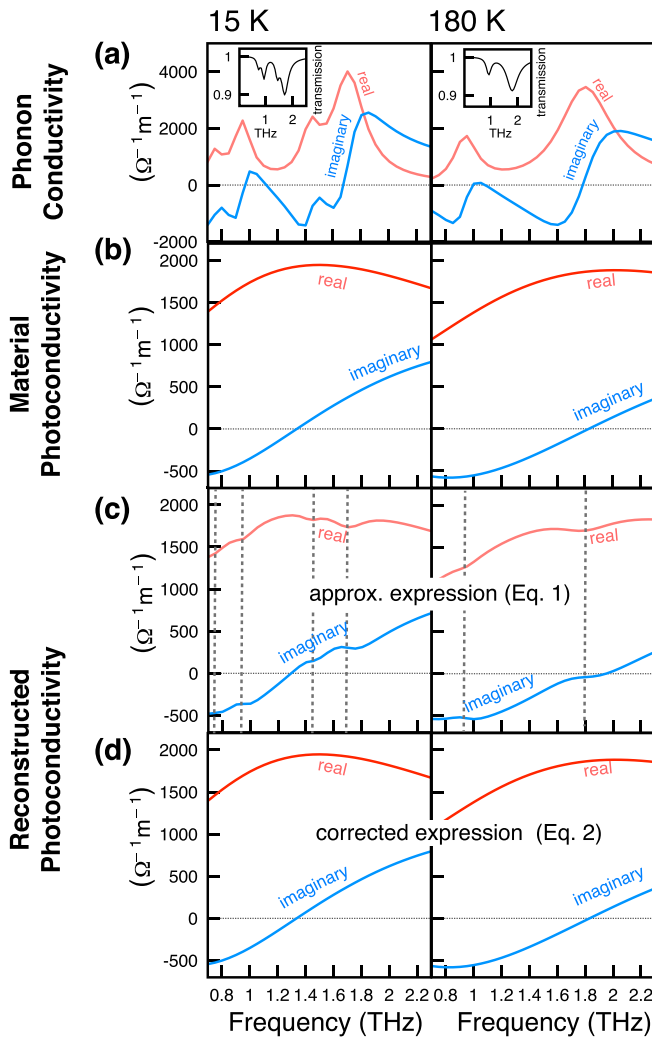


FIG. 3. Reconstructing THz photoconductivity from perovskite-like materials modeled after the experimental data at 15 and 180 K (Figs. 1(a) and 1(c)). (a) The phonon spectra are calculated from the sum of Lorentzian conductivity profiles. The corresponding THz transmission functions (inverse of the absorption) are shown in the inset (b) The photoconductivity responses of the material are given by a Drude-Smith model. (c) The thin-film approximation (Eq. (1)) shows artifacts near the phonon modes (vertical dashed lines). (d) These features are removed by introducing a correction term (Eq. (2)).

phase errors, there will still be a remnant deviation from the exact formalism as seen in Figs. 1(a), 1(c), and 1(e). Without such an error, the phonon modes now disappear from our simulation (see Fig. 3(d)) and the compensation term recovers the original photoconductivity completely.

Finally, the issue presented here is not limited only to our perovskite systems but relevant to other semiconductors that have phonon absorption in the background. Therefore, we model two general materials with Drude-like carriers with large (Figs. 4(a) and 4(b)) and small scattering rates (Figs. 4(c) and 4(d)) representing the THz photoconductivity from low and high mobility carriers, respectively. We include two phonon peaks in the background dielectric function as in the previous simulation. In both cases, using Eq. (1), the real part of the photoconductivity displays modulations at the phonon mode frequencies, similar to what we see in Fig. 3 and reported by other groups.^{5,6,10,11,17} Moreover, in the case of large scattering rate, the imaginary part of the photoconductivity shows a sign change near the phonon

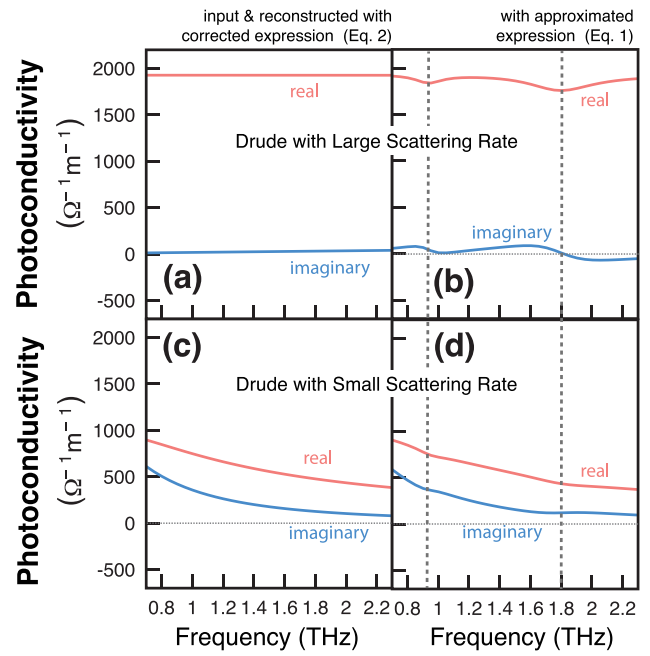


FIG. 4. A simulated material with (a) and (b) large and (c) and (d) small Drude scattering rate without Smith's term. In the former, due to the artifact, the real part of the complex photoconductivity displays modulations at the phonon mode frequencies (vertical dashed lines), while the imaginary part becomes negative leading to a possible confusion between (a) Drude-like (positive imaginary part) and (b) localized transports (negative imaginary part).

mode resonances (Fig. 4(b))—this sign change will dramatically affect the physical interpretation of the data, as a negative imaginary part of the photoconductivity usually implies the presence of localized carriers in contrast to free Drude-like carriers that have a positive imaginary part.

Both simulations also show that the phonon artifacts due to the missing correction factor appear only locally near the phonon modes (Fig. 4(b)); therefore, it will be problematic only when considering spectral features in photoconductivity. A frequency-averaged photoconductivity (or 1D-TRTS technique) used to determine the lower bound of carrier mobility and recombination rate constant^{5,6,11} does not suffer significantly from this error as the spectral averaging smooths out this phonon feature.

We have shown that features due to phonon resonances can appear spuriously over the photoconductivity spectrum when the inappropriate thin-film formula is used. A strong charge-phonon coupling might have been erroneously suggested. We present a method to circumvent this issue by the use of a more accurate thin-film approximation. Our intention is not to discount the possibility of the presence of carrier-phonon coupling in the perovskites but to send a message that a proper data analysis must be carried out before proceeding to any physical interpretation. Note that we are presenting a very common scenario, not limited to the perovskites, but including other materials that have phonon modes that coincide with the Drude-type photoconductivity below 5 THz, such as organic polymers,²⁵ DNA,^{26,27} and high-permittivity materials.

This article concludes by the derivations of the two involved thin-film formulas for the optical constants of a thin film deposited on a substrate. First, one needs to assume the complex THz electric field through the film-on-substrate

$\tilde{E}(\omega)$, as well as through the uncoated substrate as reference $\tilde{E}_{sub}(\omega)$. The resulting transmission function $\tilde{T}(\omega) \equiv \tilde{E}/\tilde{E}_{sub}$ is given by^{21,22}

$$\frac{\tilde{T}(\omega)}{\tilde{\Phi}_s(\omega)} = \frac{2\tilde{n}(\tilde{n}_{sub} + 1)e^{-i\alpha}}{(1 + \tilde{n})(\tilde{n} + \tilde{n}_{sub})e^{-i\tilde{n}\alpha} + (\tilde{n} - 1)(\tilde{n}_{sub} - \tilde{n})e^{i\tilde{n}\alpha}}, \quad (3)$$

where $\alpha \equiv \omega d/c$, \tilde{n} is a refractive index of the film, \tilde{n}_{sub} is the refractive index of the substrate, and d is the film thickness. The phase term $\tilde{\Phi}_s = \exp[-i\omega\Delta L(\tilde{n}_{sub} - 1)/c]$ takes into account the difference in the sample and reference substrate thicknesses ΔL , and c is the speed of light.

In the case of a thin film where $i\tilde{n}\alpha \ll 1$, we expand the exponential $\exp[i\tilde{n}\alpha] \approx 1 + i\tilde{n}\alpha - \tilde{n}^2\alpha^2/2$ and solve for the dielectric constant, $\tilde{n}^2 = \tilde{\epsilon}$. The numerator of Eq. (3) is expanded to first order in α , while the denominator must be expanded to second order in α , because the denominator factors $(1 + \tilde{n})(\tilde{n} + \tilde{n}_{sub})$ and $(\tilde{n} - 1)(\tilde{n}_{sub} - \tilde{n})$ are quadratic in \tilde{n} . If the second-order expansion is not included consistently, the factor $(1 - \tilde{n}^2\alpha^2/2)$ below will be missed out. The resulting expansion and taking the reciprocal result in

$$\frac{\tilde{\Phi}_s(\omega)}{\tilde{T}(\omega)} \approx \frac{1}{(1 - i\alpha)(1 + \tilde{n}_{sub})} \times \left[\left(1 - \frac{\tilde{n}^2\alpha^2}{2}\right)(1 + \tilde{n}_{sub}) - i\alpha\tilde{n}^2 - i\alpha\tilde{n}_{sub} \right]. \quad (4)$$

Next, we derive the complex optical conductivity of the thin film, $\tilde{\sigma}_{ff}^{(1)}$, from its well-known relation with \tilde{n} : $\tilde{\sigma}_{ff}^{(1)} = i\omega\epsilon_0(1 - \tilde{n}^2)$ (ff = “thin film”), to get

$$\tilde{\sigma}_{ff}^{(1)} = -\frac{\epsilon_0 c}{d} \frac{(1 + \tilde{n}_{sub})(1 - i\alpha) \left(1 - \frac{\tilde{\Phi}_s}{\tilde{T}}\right)}{1 - \frac{i\alpha}{2}(1 + \tilde{n}_{sub})} + \frac{\epsilon_0 \frac{\omega\alpha}{2}(1 + \tilde{n}_{sub})}{1 - i\frac{\alpha}{2}(1 + \tilde{n}_{sub})}, \quad (5)$$

where the superscript “(1)” denotes the expression that is expressed to first order in α . Note that the second term of Eq. (5) does not change during the transient—the substrate is chosen such that its complex refractive index is not affected by the pump pulse.

Next, we calculate the photoinduced change in the complex optical conductivity (or photoconductivity transient) from its definition, $\Delta\tilde{\sigma}_{ff}^{(1)} = \tilde{\sigma}_{ff}^{(1)} - \tilde{\sigma}_{ff,0}^{(1)}$, where the subscript “0” denotes the equilibrium (i.e., no pump) value. The equilibrium optical conductivity of the film $\tilde{\sigma}_{ff,0}^{(1)}$ can be obtained from Eq. (5) by replacing \tilde{T} with \tilde{T}_0 (the equilibrium transmission), yielding

$$\tilde{\sigma}_{ff,0}^{(1)} = -\frac{\epsilon_0 c}{d} \frac{(1 + \tilde{n}_{sub})(1 - i\alpha) \left(1 - \frac{\tilde{\Phi}_s}{\tilde{T}_0}\right)}{1 - \frac{i\alpha}{2}(1 + \tilde{n}_{sub})} + \frac{\epsilon_0 \frac{\omega\alpha}{2}(1 + \tilde{n}_{sub})}{1 - i\frac{\alpha}{2}(1 + \tilde{n}_{sub})}. \quad (6)$$

Then, we subtract Eq. (5) by Eq. (6) to write

$$\Delta\tilde{\sigma}_{ff}^{(1)} = \frac{\epsilon_0 c}{d} \frac{(1 + \tilde{n}_{sub})(1 - i\alpha)\tilde{\Phi}_s}{1 - \frac{i\alpha}{2}(1 + \tilde{n}_{sub})} \Delta\left(\frac{1}{\tilde{T}}\right), \quad (7)$$

where $\Delta\left(\frac{1}{\tilde{T}}\right) \equiv \frac{1}{\tilde{T}} - \frac{1}{\tilde{T}_0}$ can be written in the form of the electric field transients

$$\Delta\left(\frac{1}{\tilde{T}}\right) \equiv \frac{1}{\tilde{T}_0 + \Delta\tilde{T}} - \frac{1}{\tilde{T}_0} = -\frac{\Delta\tilde{E}}{\tilde{E}_0\tilde{T}_0}. \quad (8)$$

Here, $\Delta\tilde{T} = \Delta\tilde{E}/\tilde{E}_{sub} = (\tilde{E} - \tilde{E}_0)/\tilde{E}_{sub}$ is the photoinduced change in transmission function from the equilibrium value $\tilde{T}_0 = \tilde{E}_0/\tilde{E}_{sub}$, with \tilde{E}_0 being the transmitted THz electric field through the sample (film + substrate) in the absence of a pump pulse. In deriving Eq. (8), we assumed the low-excitation limit ($\Delta\tilde{E} \ll \tilde{E}_0$) and that the transmission through the reference is the same with or without pump (i.e., \tilde{E}_{sub} is a constant).

In the absence of a pump pulse, we replace, in Eq. (4), \tilde{T} by \tilde{T}_0 , and n by the equilibrium refractive index of the film n_0 , to get

$$\frac{\tilde{\Phi}_s}{\tilde{T}_0} \approx \frac{1}{(1 - i\alpha)(1 + \tilde{n}_{sub})} \times \left[\left(1 - \frac{\tilde{n}_0^2\alpha^2}{2}\right)(1 + \tilde{n}_{sub}) - i\alpha\tilde{n}_0^2 - i\alpha\tilde{n}_{sub} \right]. \quad (9)$$

Finally, after substituting Eqs. (4), (8), and (9) into Eq. (7), terms involving \tilde{T}_0 and $\tilde{\Phi}_s$ cancel out, resulting in the modified thin-film equation for THz photoconductivity

$$\begin{aligned} \Delta\tilde{\sigma}_{ff}^{(1)} &= -\epsilon_0 \frac{c}{d} \frac{\Delta\tilde{E}}{\tilde{E}_0} \frac{1 + \tilde{n}_{sub}}{1 - \frac{i\alpha(1 + \tilde{n}_{sub})}{2}} \\ &\times \left[1 - i\alpha \left(\frac{\tilde{n}_{sub} + \tilde{n}_0^2}{1 + \tilde{n}_{sub}} \right) - \frac{\tilde{n}_0^2\alpha^2}{2} \right] \\ &\approx -\epsilon_0 \frac{c}{d} \frac{\Delta\tilde{E}}{\tilde{E}_0} \left\{ (1 + \tilde{n}_{sub}) - \underbrace{\frac{i\omega d}{c} \left[\tilde{\epsilon}_{eq} - \frac{\tilde{n}_{sub}^2 + 1}{2} \right]}_{\text{1st-order correction}} \right\}, \end{aligned} \quad (10)$$

after keeping terms up to the first order in $\alpha = \omega d/c$ and using the definition of the equilibrium dielectric constant $\tilde{\epsilon}_{eq} = \tilde{n}_0^2$. This is the modified thin-film equation (Eq. (2)).

We can reduce Eq. (10) to the commonly used thin-film formula in the THz literature. For low-k dielectric materials (with small $\tilde{\epsilon}_{eq}$) on typical THz-transparent substrates like quartz or sapphire, we can neglect the first-order terms, $\frac{i\omega d}{c}(\tilde{\epsilon}_{eq} - \frac{\tilde{n}_{sub}^2 + 1}{2})$, in comparison to the zeroth-order terms $(1 + \tilde{n}_{sub})$, resulting in

$$\Delta\tilde{\sigma}_{ff} = -\epsilon_0 \frac{c}{d} (1 + \tilde{n}_{sub}) \frac{\Delta\tilde{E}}{\tilde{E}_0}, \quad (11)$$

which is Eq. (1) of the main text.

See [supplementary material](#) for a discussion of phase errors of THz measurements and material parameters used for the simulations.

This research was supported by the Theoretical and Computational Science (TaCS) Center under Computational and Applied Science for Smart Innovation Cluster (CLASSIC), Faculty of Science, KMUTT, Singapore Ministry of Education AcRF Tier 2 (MOE2015-T2-2-065), AcRF Tier 1 (RG123/14 & RF99/14) and the A*STAR Pharos Programmes (Grant No. 1527400026 & 1527000016).

- ¹T. C. Sum and N. Mathews, *Energy Environ. Sci.* **7**, 2518 (2014).
- ²C. S. Ponseca, Jr. and V. Sundstrom, *Nanoscale* **8**, 6249 (2016).
- ³C. S. Ponseca, Jr., Y. Tian, V. Sundström, and I. G. Scheblykin, *Nanotechnology* **27**, 082001 (2016).
- ⁴M. B. Johnston and L. M. Herz, *Acc. Chem. Res.* **49**, 146 (2016).
- ⁵C. Wehrenfennig, G. E. Eperon, M. B. Johnston, H. J. Snaith, and L. M. Herz, *Adv. Mater.* **26**, 1584 (2014).
- ⁶C. Wehrenfennig, M. Liu, H. J. Snaith, M. B. Johnston, and L. M. Herz, *Energy Environ. Sci.* **7**, 2269 (2014).
- ⁷C. La-o-vorakiat, T. Salim, J. Kadro, M. T. Khuc, R. Haselsberger, L. Cheng, H. Xia, G. G. Gurzadyan, H. Su, Y. M. Lam, R. A. Marcus, M.-E. Michel-Beyerle, and E. E. M. Chia, *Nat. Commun.* **6**, 7903 (2015).
- ⁸C. S. Ponseca, Jr., T. J. Savenije, M. Abdellah, K. Zheng, A. Yartsev, T. Pascher, T. Harlang, P. Chabera, T. Pullerits, A. Stepanov, J.-P. Wolf, and V. Sundström, *J. Am. Chem. Soc.* **136**, 5189 (2014).
- ⁹N. K. Noel, S. D. Stranks, A. Abate, C. Wehrenfennig, S. Guarnera, A. Haghighirad, A. Sadhanala, G. E. Eperon, S. K. Pathak, M. B. Johnston, A. Petrozza, L. M. Herz, and H. J. Snaith, *Energy Environ. Sci.* **7**, 3061 (2014).
- ¹⁰M. Karakus, S. A. Jensen, F. D'Angelo, D. Turchinovich, M. Bonn, and E. Cánovas, *J. Phys. Chem. Lett.* **6**, 4991 (2015).
- ¹¹R. L. Milot, G. E. Eperon, H. J. Snaith, M. B. Johnston, and L. M. Herz, *Adv. Funct. Mater.* **25**, 6218 (2015).
- ¹²D. Valverde-Chavez, C. S. Ponseca, C. C. Stoumpos, A. Yartsev, M. G. Kanatzidis, V. Sundström, and D. G. Cooke, *Energy Environ. Sci.* **8**, 3700 (2015).
- ¹³W. Rehman, R. L. Milot, G. E. Eperon, C. Wehrenfennig, J. L. Boland, H. J. Snaith, M. B. Johnston, and L. M. Herz, *Adv. Mater.* **27**, 7938 (2015).
- ¹⁴P. Piatkowski, B. Cohen, J. Carlito, S. Ponseca, M. Salado, S. Kazim, S. Ahmad, V. Sundstrom, and A. Douhal, *J. Phys. Chem. Lett.* **7**, 204 (2016).
- ¹⁵G. R. Yettapu, D. Talukdar, S. Sarkar, A. Swamkar, A. Nag, P. Ghosh, and P. Mandal, *Nano Lett.* **16**, 4838 (2016).
- ¹⁶C. La-o vorakiat, X. Huanxin, J. Kadro, T. Salim, D. Zhao, T. Ahmed, Y. M. Lam, J.-X. Zhu, R. A. Marcus, M.-E. Michel-Beyerle, and E. E. M. Chia, *J. Phys. Chem. Lett.* **7**, 1 (2016).
- ¹⁷C. Wehrenfennig, M. Liu, H. J. Snaith, M. B. Johnston, and L. M. Herz, *J. Phys. Chem. Lett.* **5**, 1300 (2014).
- ¹⁸A. D. Wright, C. Verdi, R. L. Milot, G. E. Eperon, M. A. Pérez-Osorio, H. J. Snaith, F. Giustino, M. B. Johnston, and L. M. Herz, *Nat. Commun.* **7**, 11755 (2016).
- ¹⁹H.-K. Nienhuys and V. Sundström, *Phys. Rev. B* **71**, 235110 (2005).
- ²⁰R. Ulbricht, E. Hendry, J. Shan, T. F. Heinz, and M. Bonn, *Rev. Mod. Phys.* **83**, 543 (2011).
- ²¹J. Petzelt, P. Kužel, I. Rychetský, A. Pashkin, and T. Ostapchuk, *Ferroelectrics* **288**, 169 (2003).
- ²²X. Zou, J. Shang, J. Leaw, Z. Luo, L. Luo, C. La-o vorakiat, L. Cheng, S. A. Cheong, H. Su, J.-X. Zhu, Y. Liu, K. P. Loh, A. H. Castro Neto, T. Yu, and E. E. M. Chia, *Phys. Rev. Lett.* **110**, 067401 (2013).
- ²³C. Kadlec, V. Skoromets, F. Kadlec, H. Němec, J. Hlinka, J. Schubert, G. Panaitov, and P. Kužel, *Phys. Rev. B* **80**, 174116 (2009).
- ²⁴G. M. Turner, M. C. Beard, and C. A. Schmittenmaer, *J. Phys. Chem. B* **106**, 11716 (2002).
- ²⁵F. A. Hegmann, O. Ostroverkhova, and D. G. Cooke, "Probing organic semiconductors with terahertz pulses," in *Photophysics of Molecular Materials: From Single Molecules to Single Crystals*, edited by G. Lanzani (Wiley, 2006).
- ²⁶D. Woolard, T. Globus, B. Gelmont, M. Bykhovskaia, A. Samuels, D. Cookmeyer, J. Hesler, T. Crowe, J. Jensen, J. Jensen, and W. Loerop, *Phys. Rev. E* **65**, 051903 (2002).
- ²⁷A. Arora, T. Q. Luong, M. Kruger, Y. J. Kim, C.-H. Nam, A. Manz, and M. Havenith, *Analyst* **137**, 575 (2012).